

# Accurate determination of the interaction between $\Lambda$ hyperons and nucleons from auxiliary field diffusion Monte Carlo calculations

D. Lonardoni\* and F. Pederiva†

*Physics Department, University of Trento, via Sommarive, 14 I-38123 Trento, Italy  
and INFN-TIFPA, Trento Institute for Fundamental Physics and Applications, Trento, Italy*

S. Gandolfi

*Theoretical Division, Los Alamos National Laboratory, Los Alamos, New Mexico 87545, USA*

(Received 3 September 2013; revised manuscript received 28 November 2013; published 21 January 2014)

**Background:** An accurate assessment of the hyperon-nucleon interaction is of great interest in view of recent observations of very massive neutron stars. The challenge is to build a realistic interaction that can be used over a wide range of masses and in infinite matter starting from the available experimental data on the binding energy of light hypernuclei. To this end, accurate calculations of the hyperon binding energy in a hypernucleus are necessary.

**Purpose:** We present a quantum Monte Carlo study of  $\Lambda$  and  $\Lambda\Lambda$  hypernuclei up to  $A = 91$ . We investigate the contribution of two- and three-body  $\Lambda$ -nucleon forces to the  $\Lambda$  binding energy.

**Method:** Ground state energies are computed solving the Schrödinger equation for nonrelativistic baryons by means of the auxiliary field diffusion Monte Carlo algorithm extended to the hypernuclear sector.

**Results:** We show that a simple adjustment of the parameters of the  $\Lambda NN$  three-body force yields a very good agreement with available experimental data over a wide range of hypernuclear masses. In some cases no experiments have been performed yet, and we give new predictions.

**Conclusions:** The newly fitted  $\Lambda NN$  force properly describes the physics of medium-heavy  $\Lambda$  hypernuclei, correctly reproducing the saturation property of the hyperon separation energy.

DOI: [10.1103/PhysRevC.89.014314](https://doi.org/10.1103/PhysRevC.89.014314)

PACS number(s): 21.80.+a, 13.75.Ev, 21.60.De, 21.60.Ka

## I. INTRODUCTION

The problem of determining a realistic interaction among hyperons and nucleons capable of reconciling the terrestrial measurements on hypernuclei and the recent observations of very massive neutron stars is still by and large unsolved. The amount of data available for nucleon-nucleon scattering [1] is enough to build satisfactory models of nuclear forces, either purely phenomenological or built on the basis of an effective field theory [2–8]. In the hyperon-nucleon sector, much less data are available [9–11], and almost nothing is known about the hyperon-hyperon interaction. The main reasons of this lack of information are the instability of hyperons in the vacuum and the impossibility of collecting hyperon-neutron and hyperon-hyperon scattering data. This implies that interaction models must be fitted mostly to binding energies (and possibly excitations) of hypernuclei.

Besides the very old emulsion data [12,13], several measurements of hypernuclear energies have become available in the last few years [14–24], both for single and double  $\Lambda$  hypernuclei. These can be used to validate or to constrain the hyperon-nucleon interactions within the framework of many-body systems. The ultimate goal is then to constrain these forces by reproducing the experimental energies of hypernuclei from light systems made of few particles up to heavier systems.

In previous work it was shown that the inclusion of a  $\Lambda NN$  interaction gives a very important repulsive contribution towards a realistic description of the saturation property of the  $\Lambda$  separation energy in medium-heavy hypernuclei [25]. In this paper, we focus on single and double  $\Lambda$  hypernuclei to study more in detail the role of  $\Lambda N$  and  $\Lambda NN$  interactions. Ground state properties of hypernuclei are here computed by means of quantum Monte Carlo (QMC) methods, and in particular by the auxiliary field diffusion Monte Carlo (AFDMC) algorithm. These methods have been shown to be very accurate in solving the many-body problem fully nonperturbatively even when the system is dominated by very strong correlations that cannot be neglected [26]. This is the case for nuclear systems.

The paper is organized as follows. In Sec. II, we introduce the Hamiltonians involved in the description of single and double  $\Lambda$  hypernuclei. Section III gives an overview of the auxiliary field diffusion Monte Carlo method with particular attention to its application to hypernuclear systems (Sec. III B). Next, in Sec. IV we report the results for single  $\Lambda$  hypernuclei (Sec. IV A) and for double  $\Lambda$  hypernuclei (Sec. IV B). Finally, in Sec. V the conclusions of our work.

## II. HAMILTONIAN

We describe nuclei and  $\Lambda$  hypernuclei with a nonrelativistic Hamiltonian that includes two- and three-body forces,

$$H_{\text{nuc}} = T_N + V_{NN} = \sum_i \frac{p_i^2}{2m_N} + \sum_{i<j} v_{ij}, \quad (1)$$

\*lonardoni@science.unitn.it

†pederiva@science.unitn.it

$$H_{\text{hyp}} = H_{\text{nuc}} + T_{\Lambda} + V_{\Lambda N} + V_{\Lambda NN} + V_{\Lambda\Lambda}$$

$$= H_{\text{nuc}} + \sum_{\lambda} \frac{p_{\lambda}^2}{2m_{\Lambda}} + \sum_{\lambda i} v_{\lambda i} + \sum_{\lambda, i < j} v_{\lambda ij} + \sum_{\lambda < \mu} v_{\lambda\mu}, \quad (2)$$

where  $A$  is the total number of baryons  $A = \mathcal{N}_N + \mathcal{N}_{\Lambda}$ , latin indices  $i, j = 1, \dots, \mathcal{N}_N$  label nucleons, and greek symbols  $\lambda, \mu = 1, \dots, \mathcal{N}_{\Lambda}$  are used for  $\Lambda$  particles. The nuclear potential is limited to a two-body interaction, while in the strange sector we adopt explicit  $\Lambda N$  and  $\Lambda NN$  interactions. In the case of double  $\Lambda$  hypernuclei, a  $\Lambda\Lambda$  force is also involved.

### A. Nucleon-nucleon interaction

The interaction between nucleons is described via the Argonne V4' and V6' two body-potentials [5], that are simplified versions of the more sophisticated Argonne V18 potential [3] obtained with a reprojected of the interaction to preserve the phase shifts of lower partial waves. The Argonne potential between two nucleons  $i$  and  $j$  is written in coordinate space as a sum of operators,

$$v_{ij} = \sum_{p=1}^n v_p(r_{ij}) \mathcal{O}_{ij}^p, \quad (3)$$

where  $n$  is the number of operators, which depends on the potential,  $v_p(r_{ij})$  are radial functions, and  $r_{ij}$  is the interparticle distance. The six operators included in the Argonne V6' potential mainly come from the one-pion exchange (OPE) between nucleons and they read

$$\mathcal{O}_{ij}^{p=1,6} = (1, \boldsymbol{\sigma}_i \cdot \boldsymbol{\sigma}_j, S_{ij}) \otimes (1, \boldsymbol{\tau}_i \cdot \boldsymbol{\tau}_j), \quad (4)$$

where  $S_{ij}$  is the usual tensor operator

$$S_{ij} = 3(\boldsymbol{\sigma}_i \cdot \hat{\mathbf{r}}_{ij})(\boldsymbol{\sigma}_j \cdot \hat{\mathbf{r}}_{ij}) - \boldsymbol{\sigma}_i \cdot \boldsymbol{\sigma}_j. \quad (5)$$

The AV4' force does not include the tensor terms  $p = 5, 6$ .

It is important to note that the above nuclear potentials do not provide the same accuracy as AV18 in fitting  $NN$  scattering data in all partial waves. In addition, three-body  $NNN$  forces are purposely disregarded for technical reasons related to the AFDMC algorithm used. As reported in Refs. [25,27], these restrictions on the nuclear potentials do not affect the main result of this work, namely the calculation of the  $\Lambda$  separation energy (the difference between the binding energy of a nucleus and the corresponding  $\Lambda$  hypernucleus), which is not significantly dependent on the specific choice of the nucleon Hamiltonian.

### B. Hyperon-nucleon interaction

To describe the interaction between the  $\Lambda$  particle and the nucleons, we adopt a class of Argonne-like interactions that have been developed starting from the 1980s by Bodmer, Usmani, and Carlson on the grounds of quantum Monte Carlo methods and have been mostly used in variational Monte Carlo calculations [28–41]. The interaction is written in coordinate space and it includes two- and three-body hyperon-nucleon components with a hard-core repulsion between baryons and a charge symmetry breaking term.

*$\Lambda N$  charge symmetric potential.* Since the  $\Lambda$  particle has isospin  $I = 0$ , there is no OPE term, the strong  $\Lambda\pi\Lambda$  vertex being forbidden due to isospin conservation. The  $\Lambda$  hyperon can exchange a pion only via a  $\Lambda\pi\Sigma$  vertex. The lowest-order  $\Lambda N$  coupling must therefore involve the exchange of two pions, with the formation of a virtual  $\Sigma$  hyperon, as illustrated in Fig. 1(a). The  $2\pi$ -exchange interaction is of intermediate range with respect to the long-range part of  $NN$  force. One-meson-exchange processes can only occur through the exchange of a  $K, K^*$  kaon pair, that contributes in exchanging strangeness between the two baryons, as shown in Fig. 1(b). The  $K, K^*$  exchange potential is short-range and it is expected to be quite weak because the  $K$  and  $K^*$  tensor contributions have opposite sign [42]. The short-range contributions are included, as in the Argonne  $NN$  interaction, by means of a Wood-Saxon repulsive potential

$$v_c(r) = W_c(1 + e^{-\frac{r-r_c}{a}})^{-1}. \quad (6)$$

The  $\Lambda N$  interaction has therefore been modeled with an Urbana-type potential [43], consistent with the available  $\Lambda p$  scattering data, with an explicit space exchange term

$$v_{\lambda i} = v_0(r_{\lambda i})(1 - \varepsilon + \varepsilon \mathcal{P}_x) + \frac{1}{4} v_{\sigma} T_{\pi}^2(r_{\lambda i}) \boldsymbol{\sigma}_{\lambda} \cdot \boldsymbol{\sigma}_i, \quad (7)$$

where  $\mathcal{P}_x$  is the  $\Lambda N$  exchange operator and  $v_0(r) = v_c(r) - \bar{v} T_{\pi}^2(r)$  is a central term. The terms  $\bar{v} = (v_s + 3v_t)/4$  and  $v_{\sigma} = v_s - v_t$  are the spin-average and spin-dependent strengths, where  $v_s$  and  $v_t$  denote singlet- and triplet-state strengths, respectively. Note that both the spin-dependent and the central radial terms contain the usual regularized OPE tensor operator  $T_{\pi}(r)$

$$T_{\pi}(r) = \left[ 1 + \frac{3}{\mu_{\pi} r} + \frac{3}{(\mu_{\pi} r)^2} \right] \frac{e^{-\mu_{\pi} r}}{\mu_{\pi} r} (1 - e^{-cr^2})^2, \quad (8)$$

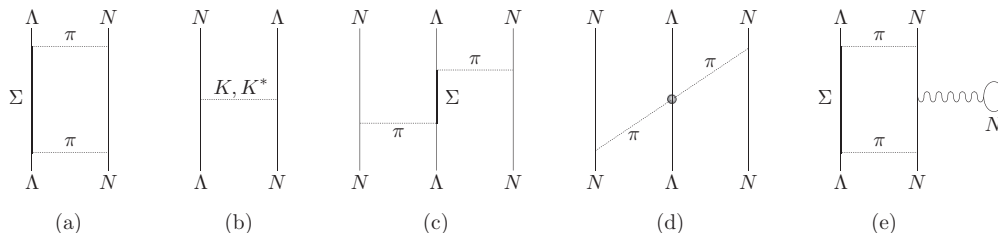


FIG. 1. Meson exchange processes between nucleons and hyperons. (a) and (b) represent the  $\Lambda N$  channels. (c)–(e) are the three-body  $\Lambda NN$  channels included in the potential by Usmani *et al.* See [41] and references therein.

TABLE I. Parameters of the  $\Lambda N$  and  $\Lambda NN$  interaction (see [41] and references therein). For  $C_P$  and  $W_D$  the variational allowed range is shown. The value of the charge-symmetry breaking parameter  $C_\tau$  is from Ref. [34].

Constant	Value	Unit
$W_c$	2137	MeV
$\bar{r}$	0.5	fm
$a$	0.2	fm
$v_s$	6.33, 6.28	MeV
$v_t$	6.09, 6.04	MeV
$\bar{v}$	6.15(5)	MeV
$v_\sigma$	0.24	MeV
$c$	2.0	fm <sup>-2</sup>
$\varepsilon$	0.1–0.38	
$C_\tau$	–0.050(5)	MeV
$C_P$	0.5–2.5	MeV
$C_S$	~1.5	MeV
$W_D$	0.002–0.058	MeV

where  $\mu_\pi$  is the pion reduced mass

$$\mu_\pi = \frac{1}{\hbar} \frac{m_{\pi^0} + 2m_{\pi^\pm}}{3}, \quad \frac{1}{\mu_\pi} \simeq 1.4 \text{ fm.} \quad (9)$$

All the parameters defining the  $\Lambda N$  potential can be found in Table I. For more details see for example Ref. [41].

*$\Lambda N$  charge symmetry breaking potential.* The  $\Lambda$ -nucleon interaction should distinguish between the nucleon isospin channels  $\Lambda p$  and  $\Lambda n$ . This is required by the experimental data, in particular the  ${}^4_\Lambda\text{H}$  and  ${}^4_\Lambda\text{He}$  ground- and excited-state energies [12], that have been reproduced in Ref. [29] by means of a phenomenological spin-dependent, charge-symmetry breaking (CSB) potential. It was found that the CSB contribution is effectively spin independent. Following Ref. [34], we can express the CSB  $\Lambda N$  interaction as

$$v_{\lambda i}^{CSB} = C_\tau T_\pi^2(r_{\lambda i}) \tau_i^z, \quad (10)$$

where  $C_\tau$  was found by the analysis of the  $A = 4$  mirror  $\Lambda$  hypernuclei and it is listed in Table I.  $C_\tau$  being negative, the  $\Lambda p$  channel becomes attractive while the  $\Lambda n$  channel is repulsive. The contribution of CSB is expected to be very small in symmetric hypernuclei (if Coulomb is neglected) but could have a significant effect in hypernuclei with a neutron (or proton) excess.

*$\Lambda NN$  potential.* In contrast to the nucleon-nucleon force, the lowest order  $\Lambda$ -nucleon interaction involves the exchange of two pions. At the same  $2\pi$ -exchange order, there are diagrams involving two nucleons and one hyperon, as shown in Figs. 1(c), 1(d), and 1(e). The first two diagrams correspond to  $P$ -wave and  $S$ -wave  $2\pi$  exchange. The last diagram represents a dispersive contribution associated with the medium modifications of the intermediate-state potentials for the  $\Sigma$ ,  $N$ ,  $\Delta$  due to the presence of the second nucleon. This term includes short-range contributions and it is expected to be repulsive due to the suppression mechanism associated with the  $\Lambda N$ - $\Sigma N$  coupling [44,45].

As reported in Ref. [41], the three-body potential  $v_{\lambda ij}$  can be conveniently decomposed in the  $2\pi$ -exchange contributions  $v_{\lambda ij}^{2\pi} = v_{\lambda ij}^{2\pi,P} + v_{\lambda ij}^{2\pi,S}$  [Figs. 1(c) and 1(d)] and the spin-dependent dispersive term  $v_{\lambda ij}^D$  [Fig. 1(e)] as follows:

$$v_{\lambda ij}^{2\pi,P} = -\frac{C_P}{6} \{X_{i\lambda}, X_{\lambda j}\} \boldsymbol{\tau}_i \cdot \boldsymbol{\tau}_j, \quad (11)$$

$$v_{\lambda ij}^{2\pi,S} = C_S Z(r_{\lambda i}) Z(r_{\lambda j}) \boldsymbol{\sigma}_i \cdot \hat{\mathbf{r}}_{i\lambda} \boldsymbol{\sigma}_j \cdot \hat{\mathbf{r}}_{j\lambda} \boldsymbol{\tau}_i \cdot \boldsymbol{\tau}_j, \quad (12)$$

$$v_{\lambda ij}^D = W_D T_\pi^2(r_{\lambda i}) T_\pi^2(r_{\lambda j}) \left[ 1 + \frac{1}{6} \boldsymbol{\sigma}_\lambda \cdot (\boldsymbol{\sigma}_i + \boldsymbol{\sigma}_j) \right]. \quad (13)$$

The function  $T_\pi(r)$  is the same as in Eq. (8), while the  $X_{\lambda i}$  and  $Z(r)$  are defined by

$$X_{\lambda i} = Y_\pi(r_{\lambda i}) \boldsymbol{\sigma}_\lambda \cdot \boldsymbol{\sigma}_i + T_\pi(r_{\lambda i}) S_{\lambda i}, \quad (14)$$

$$Z(r) = \frac{\mu_\pi r}{3} [Y_\pi(r) - T_\pi(r)], \quad (15)$$

where

$$Y_\pi(r) = \frac{e^{-\mu_\pi r}}{\mu_\pi r} (1 - e^{-cr^2}) \quad (16)$$

is the regularized Yukawa potential and  $S_{\lambda i}$  is the same tensor operator as in Eq. (5). The range of parameters  $C_P$ ,  $C_S$ , and  $W_D$  can be found in Table I. It is important to note that the three-body  $\Lambda NN$  interaction has been used in variational Monte Carlo calculations for single  $\Lambda$  hypernuclei ( ${}^3_\Lambda\text{H}$  [30,33],  ${}^4_\Lambda\text{H}$  and  ${}^4_\Lambda\text{He}$  [29,30,33,35],  ${}^5_\Lambda\text{He}$  [30,33–36,39,41,46],  ${}^9_\Lambda\text{Be}$  [28,32],  ${}^{13}_\Lambda\text{C}$  [28], and  ${}^{17}_\Lambda\text{O}$  [31,46]) and double  $\Lambda$  hypernuclei ( ${}^4_{\Lambda\Lambda}\text{H}$ ,  ${}^5_{\Lambda\Lambda}\text{H}$ ,  ${}^5_{\Lambda\Lambda}\text{He}$  [38], and  ${}^6_{\Lambda\Lambda}\text{He}$  [37,38,40]), but no unique set of parameters has been set so far.

We stress the fact that, unlike the nucleon sector, both the two- and three-body hyperon-nucleon interactions are of the same  $2\pi$ -exchange order. In addition, the mass of the intermediate excited state  $\Sigma$  compared to the  $\Lambda$  is much smaller than in the pure nucleonic case, where the difference between the nucleon and the  $\Delta$  resonance is much larger. The  $\Lambda NN$  interaction should therefore be considered necessary in addition to the  $\Lambda N$  force in any consistent theoretical calculation involving a  $\Lambda$ .

### C. Hyperon-Hyperon interaction

For the  $\Lambda\Lambda$  potential, we follow the guide lines adopted in the three- and four-body cluster models for double  $\Lambda$  hypernuclei [47,48], which were also used in Faddeev-Yakubovsky calculations for light double  $\Lambda$  hypernuclei [49] and in variational calculations on  ${}^4_{\Lambda\Lambda}\text{H}$  [38,50],  ${}^5_{\Lambda\Lambda}\text{H}$  and  ${}^5_{\Lambda\Lambda}\text{He}$  [38,51], and  ${}^6_{\Lambda\Lambda}\text{He}$  [37,38,40,51], with different parametrizations.

The employed effective interaction is a low-energy phase equivalent Nijmegen interaction represented by a sum of three Gaussians:

$$v_{\lambda\mu} = \sum_{k=1}^3 (v_0^{(k)} + v_\sigma^{(k)} \boldsymbol{\sigma}_\lambda \cdot \boldsymbol{\sigma}_\mu) e^{-\mu^{(k)} r_{\lambda\mu}^2}. \quad (17)$$

The most recent parametrization of the potential (see Table II), has been fitted to simulate the  $\Lambda\Lambda$  sector of the Nijmegen F

TABLE II. Parameters for the one-boson exchange potential simulating the  $\Lambda\Lambda$  interaction. Depths  $v_0^{(k)}$  and  $v_\sigma^{(k)}$  (MeV) for each size parameter  $\mu^{(k)}$  (fm $^{-2}$ ) [48].

$\mu^{(k)}$	0.555	1.656	8.163
$v_0^{(k)}$	-10.67	-93.51	4884
$v_\sigma^{(k)}$	0.0966	16.08	915.8

(NF) interaction [52–54]. The NF model is the simplest among the Nijmegen models with a scalar nonet, which seems to be more appropriate than the versions including only a scalar singlet in order to reproduce the weak binding energy indicated by the NAGARA event [16]. The components  $k = 1, 2$  of the above Gaussian potential are determined so as to simulate the  $\Lambda\Lambda$  sector of NF, and the strength of the part for  $k = 3$  is adjusted so as to reproduce the  ${}_{\Lambda\Lambda}^6\text{He}$  NAGARA experimental double  $\Lambda$  separation energy of  $7.25 \pm 0.19^{+0.18}_{-0.11}$  MeV. In 2010, Nakazawa reported a new, more precise determination of  $B_{\Lambda\Lambda} = 6.93 \pm 0.16$  MeV for  ${}_{\Lambda\Lambda}^6\text{He}$  [20], obtained via the  $\Xi^-$  hyperon capture at rest reaction in a hybrid emulsion. This value has been recently revised to  $B_{\Lambda\Lambda} = 6.91 \pm 0.16$  MeV by the E373 (KEK-PS) Collaboration [23]. No references were found about the refitting of the  $\Lambda\Lambda$  Gaussian potential on the more recent experimental result, which is in any case compatible with the NAGARA event. We therefore use the original parametrization of Ref. [48].

### III. METHOD

#### A. Auxiliary field DMC method for nuclei

The auxiliary field diffusion Monte Carlo (AFDMC) method was introduced by Schmidt and Fantoni [55] as an extension of the usual diffusion Monte Carlo (DMC) method to deal in an efficient way with spin/isospin-dependent Hamiltonians. The standard DMC projects out the ground state of the system by starting from a trial wave function not orthogonal to the true ground state. By sampling configurations of the system in coordinate-spin-isospin space, the trial wave function is propagated in imaginary-time  $\tau$ . Expectation values are computed averaging over the sampled configurations in the  $\tau \rightarrow \infty$  limit, for which the evolved state approaches the ground state of the Hamiltonian.

In nuclear Hamiltonians, the potential contains quadratic spin and isospin operators, so the many-body wave function cannot be written as a product of single-particle, spin-isospin states. The number of components in the propagated wave function grows exponentially with  $A$  and thus it quickly becomes computationally intractable. Standard DMC calculations for nuclei are in fact limited up to 12 nucleons [56–58] or 16 neutrons [59].

The idea of the AFDMC method consists of reducing the quadratic spin-isospin operators into linear terms in the propagator. The starting point is to recast the Argonne V6- and V4-potentials in spin-isospin independent and

spin-isospin dependent components, the latter of the form

$$\begin{aligned}
 V_{NN} = & \frac{1}{2} \sum_{i \neq j} \sum_{\gamma} \tau_{i\gamma} A_{ij}^{[\tau]} \tau_{j\gamma} \\
 & + \frac{1}{2} \sum_{i \neq j} \sum_{\alpha\beta} \sigma_{i\alpha} A_{i\alpha,j\beta}^{[\sigma]} \sigma_{j\beta} \\
 & + \frac{1}{2} \sum_{i \neq j} \sum_{\alpha\beta\gamma} \tau_{i\gamma} \sigma_{i\alpha} A_{i\alpha,j\beta}^{[\sigma\tau]} \sigma_{j\beta} \tau_{j\gamma}. \quad (18)
 \end{aligned}$$

The matrices  $A$  are real and symmetric with zero diagonals and contain proper combinations of the components of AV6 and AV4 (latin indices are used for the nucleons, greek ones refer to the Cartesian components of the operators)

$$\begin{aligned}
 A_{ij}^{[\tau]} &= v_2(r_{ij}), \\
 A_{i\alpha,j\beta}^{[\sigma]} &= v_3(r_{ij})\delta_{\alpha\beta} + v_5(r_{ij})(3\hat{r}_{ij}^\alpha \hat{r}_{ij}^\beta - \delta_{\alpha\beta}), \quad (19) \\
 A_{i\alpha,j\beta}^{[\sigma\tau]} &= v_4(r_{ij})\delta_{\alpha\beta} + v_6(r_{ij})(3\hat{r}_{ij}^\alpha \hat{r}_{ij}^\beta - \delta_{\alpha\beta}).
 \end{aligned}$$

By diagonalizing such matrices it is possible to write the quadratic operators of Eq. (4) in terms of the eigenvectors of the matrices  $A$ . In the  $\sigma$  channel we define for example

$$\mathcal{O}_n^{[\sigma]} = \sum_{j\beta} \sigma_{j\beta} \psi_{n,j\beta}^{[\sigma]}, \quad (20)$$

where

$$\sum_{j\beta} A_{i\alpha,j\beta}^{[\sigma]} \psi_{n,j\beta}^{[\sigma]} = \lambda_n^{[\sigma]} \psi_{n,i\alpha}^{[\sigma]}. \quad (21)$$

Given the nucleon-nucleon spin-isospin dependent interaction in this form, we can write the imaginary time propagator by means of the Hubbard-Stratonovich (HS) transformation

$$e^{-\frac{1}{2}\tau \lambda_n (\mathcal{O}_n)^2} = \frac{1}{\sqrt{2\pi}} \int dx_n e^{-\frac{x_n^2}{2}} e^{\sqrt{-\tau \lambda_n} x_n \mathcal{O}_n}. \quad (22)$$

The newly introduced  $x_n$  variables, called *auxiliary fields*, are sampled to evaluate the integral of Eq. (22). The linearized propagator has the effect of rotating the spin-isospin components of each single nucleon. This eventually recovers the action of the quadratic spin-isospin operators on the trial wave function containing all the possible good spin-isospin states. The procedure described reduces the dependence to the number of operations needed to evaluate the trial wave function from exponential to polynomial in the number of nucleons. The price to pay is the additional computational cost due to the diagonalization of the  $A$  matrices and the sampling of the integral over auxiliary fields. In any case, there is a net gain in computational time, the total number of AFDMC operations being at most proportional to  $A^3$ .

The details of the AFDMC algorithm for nuclei and neutron matter can be found in Refs. [60–62], where the adopted nuclear wave function, the computation of expectation values, and the approximations used to overcome the Fermion sign problem are discussed in detail.

### B. Auxiliary field DMC method for hypernuclei

*Hypernuclear wave function.* The starting point of all DMC methods is the set up of the trial wave function. The  $\Lambda$  particle is distinguishable from the nucleons so, to describe single and double  $\Lambda$  hypernuclei, we write a factorized trial wave function of the form

$$\psi_T(R, S) = \psi_T^N(R_N, S_N) \psi_T^\Lambda(R_\Lambda, S_\Lambda), \quad (23)$$

where  $R = \{R_N, R_\Lambda\}$  and  $S = \{S_N, S_\Lambda\}$  with  $R_p = \{\mathbf{r}_1, \dots, \mathbf{r}_{N_p}\}$  and  $S_p = \{s_1, \dots, s_{N_p}\}$ ,  $p = N, \Lambda$ . The two components of  $\psi_T$  are chosen to be of the same form as in Refs. [61],

$$\psi_T^p(R_p, S_p) = \left[ \prod_{i < j} f_{ij} \right]_p \mathcal{A} \left[ \prod_i \varphi_i(\mathbf{r}_i - \mathbf{r}_{CM}, s_i) \right], \quad (24)$$

where  $\mathcal{A}$  is an antisymmetrization operator,  $\mathbf{r}_{CM}$  is the center of mass of the hypernucleus, and  $\varphi_i$  are single-particle space and spin-isospin orbitals, built from combinations of radial functions, spherical harmonics, and spinors. Radial orbitals are the solutions of the self-consistent Hartree-Fock problem with the Skyrme effective interactions of Ref. [63]. For the  $\Lambda$  particle, we assume the neutron  $1s_{1/2}$  radial function. Spinors are defined as four-component complex vectors for the nucleons and two-component complex vectors for the  $\Lambda$  particles:

$$s_i^N = \begin{pmatrix} a_i \\ b_i \\ c_i \\ d_i \end{pmatrix} = a_i |p \uparrow\rangle + b_i |p \downarrow\rangle + c_i |n \uparrow\rangle + d_i |n \downarrow\rangle, \quad (25)$$

$$s_i^\Lambda = \begin{pmatrix} u_i \\ v_i \end{pmatrix} = u_i |\Lambda \uparrow\rangle + v_i |\Lambda \downarrow\rangle. \quad (26)$$

The functions  $f_{ij}$  are symmetric and spin independent Jastrow correlation functions, solutions of the Schrödinger-like equation for  $f_{ij}(r < d)$ ,

$$-\frac{\hbar^2}{2\mu_{ij}} \nabla^2 f_{ij}(r) + \eta v_{ij}^c(r) f_{ij}(r) = \xi f_{ij}(r), \quad (27)$$

where  $v_{ij}^c(r)$  is the spin-independent part of the two-body interaction,  $\mu_{ij} = m_p/2$  the reduced mass of the pair, and  $\eta$  and the healing distance  $d$  are variational parameters. For distances  $r \geq d$ , we impose  $f_{ij}(r) = 1$ . The role of  $f_{ij}$  functions is to include the short-range correlations in the trial wave function. In the AFDMC algorithm the effect is simply a reduction of the overlap between pairs of particles, with the reduction of the energy variance. Since there is no change in the phase of the wave function, the  $f_{ij}$  do not influence the computed energy value in projection methods.

With the presented wave function, we consider nucleons and hyperons as distinct particles. In this way, it is not possible to include the  $\Lambda N$  exchange term of Eq. (7) directly in the propagator, because it mixes hyperon and nucleon states. The complete treatment of this factor would require an enlarged hyperon-nucleon isospin space, which at present has not yet been developed. A perturbative analysis of the  $v_0(r)\varepsilon(\mathcal{P}_x - 1)$  term is, however, possible as described in Ref. [25].

*Algorithm.* The idea of the standard AFDMC method can be easily extended to  $\Lambda$  hypernuclear systems with the interactions described in Secs. II B and II C. Consider the hypernuclear potentials of Eqs. (7), (10), (11)–(13), and (17), and assume the notations

$$\begin{aligned} T_{\lambda i} &= T_\pi(r_{\lambda i}), \\ Y_{\lambda i} &= Y_\pi(r_{\lambda i}), \\ Q_{\lambda i} &= Y_{\lambda i} - T_{\lambda i}. \end{aligned} \quad (28)$$

In analogy with the nucleon-nucleon  $A$  matrices of Eqs. (19), we can define the following hyperon-nucleon and hyperon-hyperon matrices (greek  $\lambda, \mu$  indices indicate the  $\Lambda$  particles)

$$B_{\lambda i}^{[\sigma]} = \frac{1}{4} v_\sigma T_{\lambda i}, \quad (29)$$

$$C_{\lambda i}^{[\sigma]} = \frac{1}{3} W_D \sum_{j, j \neq i} T_{\lambda i}^2 T_{\lambda j}^2, \quad (30)$$

$$\begin{aligned} C_{i\alpha, j\beta}^{[\sigma\tau]} &= \sum_\lambda \left\{ -\frac{1}{3} C_P Q_{\lambda i} Q_{\lambda j} \delta_{\alpha\beta} - C_P Q_{\lambda j} T_{\lambda i} \hat{r}_{i\lambda}^\alpha \hat{r}_{i\lambda}^\beta \right. \\ &\quad - C_P Q_{\lambda i} T_{\lambda j} \hat{r}_{j\lambda}^\alpha \hat{r}_{j\lambda}^\beta + \left[ \frac{1}{9} C_S \mu_\pi^2 Q_{\lambda i} Q_{\lambda j} |r_{i\lambda}| |r_{j\lambda}| \right. \\ &\quad \left. \left. - 3 C_P T_{\lambda i} T_{\lambda j} \left( \sum_\delta \hat{r}_{i\lambda}^\delta \hat{r}_{j\lambda}^\delta \right) \right] \hat{r}_{i\lambda}^\alpha \hat{r}_{j\lambda}^\beta \right\}, \end{aligned} \quad (31)$$

$$D_{\lambda\mu}^{[\sigma]} = \sum_{k=1}^3 v_\sigma^{(k)} e^{-\mu^{(k)} r_{\lambda\mu}^2}. \quad (32)$$

In such a way it is possible to recast the  $\Lambda N$ ,  $\Lambda NN$ , and  $\Lambda\Lambda$  interactions so that they contain at most two-body operators in the hyperon-nucleon extended space

$$V_{\Lambda N} = \sum_{\lambda i} \sum_\alpha \sigma_{\lambda\alpha} B_{\lambda i}^{[\sigma]} \sigma_{i\alpha} + \tilde{V}_{\Lambda N}, \quad (33)$$

$$V_{\Lambda NN}^{2\pi} = \frac{1}{2} \sum_{i \neq j} \sum_{\alpha\beta\gamma} \tau_{i\gamma} \sigma_{i\alpha} C_{i\alpha, j\beta}^{[\sigma\tau]} \sigma_{j\beta} \tau_{j\gamma}, \quad (34)$$

$$V_{\Lambda NN}^D = \frac{1}{2} \sum_{\lambda i} \sum_\alpha \sigma_{\lambda\alpha} C_{\lambda i}^{[\sigma]} \sigma_{i\alpha} + \tilde{V}_{\Lambda NN}, \quad (35)$$

$$V_{\Lambda\Lambda} = \frac{1}{2} \sum_{\lambda \neq \mu} \sum_\alpha \sigma_{\lambda\alpha} D_{\lambda\mu}^{[\sigma]} \sigma_{\mu\alpha} + \tilde{V}_{\Lambda\Lambda}, \quad (36)$$

where  $\tilde{V}_{\Lambda N}$ ,  $\tilde{V}_{\Lambda NN}$ , and  $\tilde{V}_{\Lambda\Lambda}$  include all the spin-isospin independent and the linear  $\mathcal{P}_x, \tau_i^z$  terms

$$\begin{aligned} \tilde{V}_{\Lambda N} &= \sum_{\lambda i} v_0(r_{\lambda i})(1 - \varepsilon) + \sum_{\lambda i} v_0(r_{\lambda i}) \varepsilon \mathcal{P}_x \\ &\quad + \sum_{\lambda i} C_\tau T_\pi^2(r_{\lambda i}) \tau_i^z, \\ \tilde{V}_{\Lambda NN} &= \sum_{\lambda, i < j} W_D T_\pi^2(r_{\lambda i}) T_\pi^2(r_{\lambda j}), \\ \tilde{V}_{\Lambda\Lambda} &= \sum_{\lambda < \mu} \sum_{k=1}^3 v_0^{(k)} e^{-\mu^{(k)} r_{\lambda\mu}^2}. \end{aligned} \quad (37)$$

All the remaining terms of Eqs. (33)–(36) consist of two-body spin-isospin operators of exactly the same type as those of Eqs. (18).

The algorithm follows then the nuclear version with the sampling of the coordinates, which now contains also the  $\Lambda$  particles, and of the auxiliary fields, one for each linearized operator. The application of the propagator of Eq. (22) has the effect of rotating the spinors of nucleons and  $\Lambda$ s. The strategy adopted in order to control the Fermion sign problem and reduce the variance of the estimators is the same of Refs. [60–62], with a straightforward extension to the enlarged hyperon-nucleon space.

The structure of the AFDMC algorithm for  $\Lambda$  hypernuclei closely follows the usual AFDMC procedure:

- (i) Sample the nucleons and  $\Lambda$ 's positions, spins and isospins from  $|\psi_T(R, S)|^2$ , using the Metropolis Monte Carlo method.
- (ii) Propagate the spatial degrees of freedom as in the usual diffusion Monte Carlo with a drifted Gaussian for a small time step.
- (iii) For each set of generalized coordinates (*walker*), build and diagonalize the potential matrices  $A$ ,  $B$ ,  $C$ , and  $D$ .
- (iv) Loop over the eigenvectors, sampling the corresponding auxiliary fields and rotating the spinors.
- (v) Apply the fixed phase prescription and evaluate the estimator contributions to averages for the calculation of expectation values.
- (vi) Iterate from 2 to 5 as long as necessary until convergence of the energy is reached. Error bars on expectation values are then estimated by means of block averages and the analysis of autocorrelations on data blocks.

## IV. RESULTS AND DISCUSSION

### A. Single $\Lambda$ hypernuclei

A direct comparison of energy calculations with experimental results is given for the  $\Lambda$  separation energy, defined as

$$B_\Lambda(^A\Lambda Z) = E(^{A-1}Z) - E(^A\Lambda Z), \quad (38)$$

where  $E$  is the energy of the system, i.e. the ground state expectation value of the Hamiltonian,

$$E(\kappa) = \frac{\langle \psi_\kappa^0 | H_\kappa | \psi_\kappa^0 \rangle}{\langle \psi_\kappa^0 | \psi_\kappa^0 \rangle}, \quad \kappa = \text{nuc, hyp.} \quad (39)$$

The computation of  $B_\Lambda$  thus involves the calculation of the energy of the nucleus  $^{A-1}Z$  and the corresponding hypernucleus  $^A\Lambda Z$ . The nuclear wave function is the same as in Eq. (24) with the spinor of Eq. (25). As reported in Refs. [25,27], the  $\Lambda$  separation energy is not sensitive to the details of the nuclear interactions. On the grounds of this observation, we adopt the nuclear potential  $AV4'$  for both nuclei and hypernuclei in the present work. This choice makes AFDMC calculations less expensive and more stable. The resulting absolute binding energies are not comparable with experimental results, but the estimated  $B_\Lambda$  is in any case realistic.

In our previous work [25], we tackled the problem of hyperon-nucleon interaction by studying closed-shell single  $\Lambda$  hypernuclei with the inclusion of two- and three-body  $\Lambda$ -nucleon forces. The set of parameters for the  $\Lambda NN$  potential was originally taken from Ref. [46], being the choice that made the variational  $B_\Lambda$  for  $^5_\Lambda\text{He}$  and  $^{17}_\Lambda\text{O}$  compatible with the expected results. It reads

$$(I) \begin{cases} C_P = 0.60 \text{ MeV}, \\ C_S = 0.00 \text{ MeV}, \\ W_D = 0.015 \text{ MeV}. \end{cases}$$

The main outcome of the study is that the saturation property of the  $\Lambda$  binding energy is reproduced only with the inclusion of the  $\Lambda NN$  interaction. However, with the given parametrization, only a qualitative accord with the experimental results is obtained. Thus, a refitting procedure for the three-body hyperon-nucleon interaction is needed.

As reported in Ref. [41], the  $C_S$  parameter can be estimated by comparing the  $S$ -wave term of Eq. (12) with the Tucson-Melbourne model of the  $NNN$  force reported in Ref. [64]. We take the same  $C_S = 1.50$  MeV value, in order to reduce the number of fitting parameters. This choice is justified because the  $S$ -wave component of the three-body  $\Lambda NN$  interaction is sub-leading. We indeed verified that a change in the  $C_S$  value yields a variation of the total energy within statistical error bars and definitely much smaller than the variation in energy due to a change of the  $C_P$  and  $W_D$  parameters.

In Fig. 2 we report the systematic study of the  $\Lambda$  separation energy of  $^5_\Lambda\text{He}$  as a function of both  $W_D$  and  $C_P$ . Solid black dots are the AFDMC results. The red grid represents the experimental  $B_\Lambda = 3.12(2)$  MeV [12]. The dashed yellow curve follows the set of parameters reproducing the expected  $\Lambda$  separation energy. The same curve is also reported in Fig. 3 (red band with black dots and error bars), that is a projection of Fig. 2 on the  $W_D$ - $C_P$  plane. The dashed box represents the  $W_D$  and  $C_P$  domain of the previous picture. For comparison, the variational results of Ref. [41] are also reported. Green curves are the results for  $\bar{v} = 6.15$  MeV and  $v_\sigma = 0.24$  MeV, blue ones for  $\bar{v} = 6.10$  MeV and  $v_\sigma = 0.24$  MeV. Dashed,

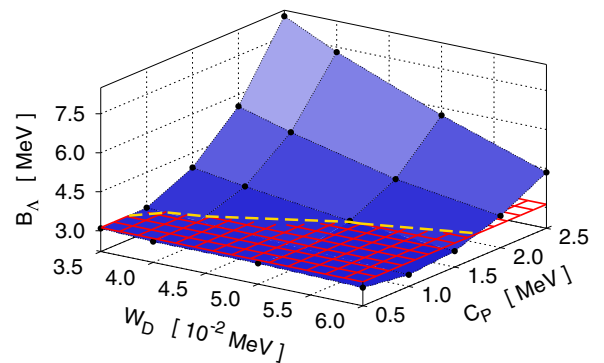


FIG. 2. (Color online)  $\Lambda$  separation energy for  $^5_\Lambda\text{He}$  as a function of strengths  $W_D$  and  $C_P$  of the three-body  $\Lambda NN$  interaction. The red grid represents the experimental  $B_\Lambda = 3.12(2)$  MeV [12]. The dashed yellow curve is the interception between the expected result and the  $B_\Lambda$  surface in the  $W_D$ - $C_P$  parameter space. Statistical error bars on AFDMC results (solid black dots) are of the order of 0.10–0.15 MeV.

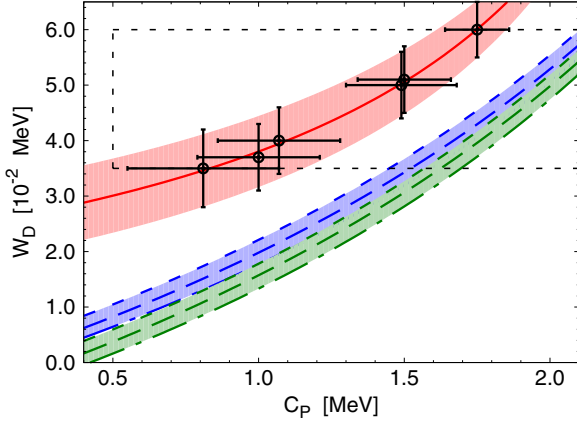


FIG. 3. (Color online) Projection of Fig. 2 on the  $W_D$ - $C_P$  plane. Error bars come from a realistic conservative estimate of the uncertainty in the determination of the parameters due to the statistical errors of the Monte Carlo calculations. Blue and green dashed, long-dashed, and dot-dashed lines (lower curves) are the variational results of Ref. [41] for different  $\varepsilon$  and  $\bar{v}$  (two-body  $\Lambda N$  potential). The dashed box corresponds to the parameter domain of Fig. 2. Black dots and the red band (upper curve) are the projected interception describing the possible set of parameters reproducing the experimental  $B_\Lambda$ .

long-dashed, and dot-dashed lines correspond respectively to  $\varepsilon = 0.1, 0.2$ , and  $0.3$ .

In our calculations, we have not considered different combinations for the parameters of the two-body  $\Lambda N$  interaction, focusing on the three-body part. We have thus kept fixed  $\bar{v}$  and  $v_\sigma$  to the same values of the green curves of Fig. 3 (see Table I for the detailed list of constants). Moreover, in the present work we have set  $\varepsilon = 0$  for all the studied hypernuclei due to the impossibility of exactly including the  $\mathcal{P}_x$  exchange operator in the propagator. However, from a perturbative analysis, the net effect of the  $v_0(r)\varepsilon(\mathcal{P}_x - 1)$  term on the hyperon separation energy within the statistical errors of the Monte Carlo calculation, seems to be the same as a slight change in the strength of the central  $\Lambda N$  potential.

Starting from the analysis of the results in the  $W_D$ - $C_P$  space for  ${}^5_\Lambda\text{He}$ , we performed simulations for the next closed-shell hypernucleus  ${}^{17}_\Lambda\text{O}$ . Using the parameters in the red band of Fig. 3 we identified a parametrization able to reproduce the experimental  $B_\Lambda$  for both  ${}^5_\Lambda\text{He}$  and  ${}^{17}_\Lambda\text{O}$  at the same time, namely

$$(II) \begin{cases} C_P = 1.00 \text{ MeV}, \\ C_S = 1.50 \text{ MeV}, \\ W_D = 0.035 \text{ MeV}. \end{cases}$$

Given the set (II), the  $\Lambda$  separation energy of closed-shell and open-shell single  $\Lambda$  hypernuclei has been calculated in a mass range  $3 \leq A \leq 91$ . The closed-shell hypernuclei are the same of Ref. [25]. The results are summarized in Fig. 4, where we report  $B_\Lambda$  as a function of  $A^{-2/3}$ , and as a function of  $A$  in the inset. Solid green dots are the available experimental data, empty symbols the AFDMC results. The blue curve is obtained using only the two-body hyperon-nucleon interaction in addition to the nuclear AV4' potential. The red curve refers

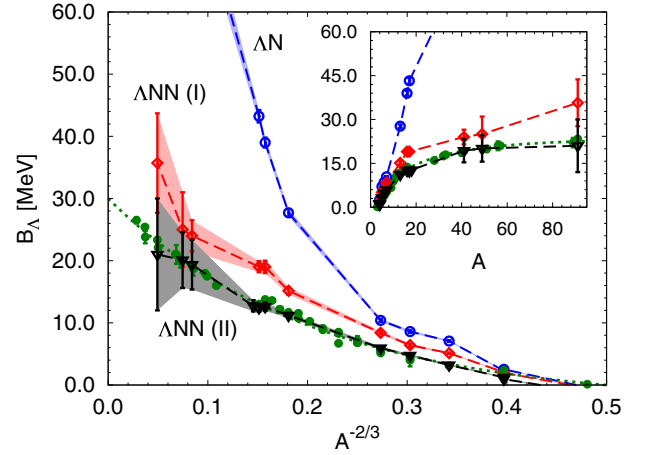


FIG. 4. (Color online)  $\Lambda$  separation energy as a function of  $A^{-2/3}$ . Solid green dots (dashed curve) are the available  $B_\Lambda$  experimental or semiempirical values. Empty blue dots (upper banded curve) refer to the AFDMC results for the two-body  $\Lambda N$  interaction alone. Empty red diamonds (middle banded curve) and empty black triangles (lower banded curve) are the results with the inclusion also of the three-body hyperon-nucleon force, respectively for the set of parameters (I) and (II). In the inset, the same data plotted as a function of  $A$ .

to the results for the same systems when also the three-body  $\Lambda NN$  interaction with the old set of parameters (I) is included. The black lower curve shows the results obtained by including the three-body hyperon-nucleon interaction described by the new parametrization (II). A detailed comparison between numerical results and experiments for the hyperon-separation energy can be found in Table III.

TABLE III.  $\Lambda$  separation energies (in MeV) obtained using the two-body plus three-body hyperon-nucleon interaction with the set of parameters (II). The results already include the CSB contribution. In the last column are the expected  $B_\Lambda$  values. No experimental data for  $A = 17, 18, 41, 49, 91$  exist. For  ${}^{17}_\Lambda\text{O}$  the reference separation energy is a semiempirical value. For  $A = 41, 49, 91$  the experimental hyperon binding energies are those of the nearest hypernuclei  ${}^{40}_\Lambda\text{Ca}$ ,  ${}^{51}_\Lambda\text{V}$ , and  ${}^{89}_\Lambda\text{Y}$  respectively.

System	AFDMC $B_\Lambda$	Expt. $B_\Lambda$
${}^3_\Lambda\text{H}$	-1.22(15)	0.13(5) [12]
${}^4_\Lambda\text{H}$	0.95(9)	2.04(4) [12]
${}^4_\Lambda\text{He}$	1.22(9)	2.39(3) [12]
${}^5_\Lambda\text{He}$	3.22(14)	3.12(2) [12]
${}^6_\Lambda\text{He}$	4.76(20)	4.25(10) [12]
${}^7_\Lambda\text{He}$	5.95(25)	5.68(28) [22]
${}^{13}_\Lambda\text{C}$	11.2(4)	11.69(12) [13]
${}^{16}_\Lambda\text{O}$	12.6(7)	12.42(41) [65]
${}^{17}_\Lambda\text{O}$	12.4(6)	13.0(4) [31]
${}^{18}_\Lambda\text{O}$	12.7(9)	
${}^{41}_\Lambda\text{Ca}$	19(4)	18.7(1.1) [14]
${}^{49}_\Lambda\text{Ca}$	20(5)	19.97(13) [66]
${}^{91}_\Lambda\text{Zr}$	21(9)	23.11(10) [66]

TABLE IV.  $\Lambda$  separation energies (in MeV) for the  $A = 4$  mirror  $\Lambda$  hypernuclei with (fourth column) and without (third column) the inclusion of the charge symmetry breaking term. In the last column the difference in the separation energy induced by the CSB interaction. First and second rows refer to different set of parameters for the  $\Lambda NN$  interaction, while the last row is the experimental result.

Parameters	System	$B_{\Lambda}^{\text{sym}}$	$B_{\Lambda}^{\text{CSB}}$	$\Delta B_{\Lambda}^{\text{CSB}}$
Set (I)	${}^4_{\Lambda}\text{H}$	1.97(11)	1.89(9)	0.24(12)
	${}^4_{\Lambda}\text{He}$	2.02(10)	2.13(8)	
Set (II)	${}^4_{\Lambda}\text{H}$	1.07(8)	0.95(9)	0.27(13)
	${}^4_{\Lambda}\text{He}$	1.07(9)	1.22(9)	
Expt. [12]	${}^4_{\Lambda}\text{H}$		2.04(4)	0.35(5)
	${}^4_{\Lambda}\text{He}$		2.39(3)	

For systems with  $A \geq 5$ , all the  $\Lambda$  separation energies are compatible with the expected results, where available. For  $A < 5$  our results are more than 1 MeV off from experimental data. For  ${}^3_{\Lambda}\text{H}$ , the  $\Lambda$  separation energy is even negative, meaning that the hypernucleus is less bound than the corresponding nucleus  ${}^2\text{H}$ . We can ascribe this discrepancy to the lack of accuracy of our nucleonic wave function. Moreover, the single-particle orbitals might need to be changed when the  $\Lambda$  is added to the nucleus. This effect is expected to be much less important for heavier hypernuclei where bulk effects dominate over the surface. A study of these systems within a few-body method might solve this issue.

The effect of the CSB potential has been studied for the  $A = 4$  mirror hypernuclei. As reported in Table IV, without the CSB term there is no difference in the  $\Lambda$  binding energy of  ${}^4_{\Lambda}\text{H}$  and  ${}^4_{\Lambda}\text{He}$ . When CSB is active, a splitting appears due to the different behavior of the  $\Lambda p$  and  $\Lambda n$  channels. The strength of the difference  $\Delta B_{\Lambda}^{\text{CSB}}$  is independent on the parameters of the three-body  $\Lambda NN$  interaction and it is compatible with the experimental result [12].

The same CSB potential of Eq. (10) has been included in the study of hypernuclei for  $A > 4$ . In Table V, the difference

TABLE V. Difference (in MeV) in the hyperon separation energies induced by the CSB term for different hypernuclei. The fourth column reports the difference between the number of neutrons and protons. Results are obtained with the full two- plus three-body [set (II)] hyperon-nucleon interaction. In order to reduce the errors,  $\Delta B_{\Lambda}$  has been calculated by taking the difference between total hypernuclear binding energies, instead of the hyperon separation energies.

System	$p$	$n$	$\Delta_{np}$	$\Delta B_{\Lambda}$
${}^4_{\Lambda}\text{H}$	1	2	+1	-0.12(8)
${}^4_{\Lambda}\text{He}$	2	1	-1	+0.15(9)
${}^5_{\Lambda}\text{He}$	2	2	0	+0.02(9)
${}^6_{\Lambda}\text{He}$	2	3	+1	-0.06(8)
${}^7_{\Lambda}\text{He}$	2	4	+2	-0.18(8)
${}^{16}_{\Lambda}\text{O}$	8	7	-1	+0.27(35)
${}^{17}_{\Lambda}\text{O}$	8	8	0	+0.15(35)
${}^{18}_{\Lambda}\text{O}$	8	9	+1	-0.74(49)

in the hyperon separation energies  $\Delta B_{\Lambda} = B_{\Lambda}^{\text{CSB}} - B_{\Lambda}^{\text{sym}}$  is reported for different hypernuclei up to  $A = 18$ . The fourth column shows the difference between the number of neutrons and protons  $\Delta_{np} = \mathcal{N}_n - \mathcal{N}_p$ . For the symmetric hypernuclei  ${}^5_{\Lambda}\text{He}$  and  ${}^{17}_{\Lambda}\text{O}$  the CSB interaction has no effect, this difference being zero. In the systems with neutron excess ( $\Delta_{np} > 0$ ), the effect of the CSB consists in decreasing the hyperon separation energy compared to the charge symmetric case. When  $\Delta_{np}$  becomes negative,  $\Delta B_{\Lambda} > 0$  due to the attraction induced by the CSB potential in the  $\Lambda p$  channel, producing more bound hypernuclei. These effects are in any case rather small and they become almost negligible compared to the statistical errors on  $B_{\Lambda}$  when the number of baryons becomes large enough ( $A > 16$ ).

Single-particle densities can be computed in Monte Carlo calculations by considering the expectation value of the density operator

$$\hat{\rho}_{\kappa}(r) = \sum_i \delta(r - r_i), \quad \kappa = N, \Lambda, \quad (40)$$

where  $i$  is the single particle index running over nucleons for  $\rho_N = \langle \hat{\rho}_N \rangle$  or hyperons for  $\rho_{\Lambda} = \langle \hat{\rho}_{\Lambda} \rangle$ . The correct estimator for positive defined operators  $\mathcal{O}$  different from the total Hamiltonian is obtained starting from the mixed DMC result and the variational one via the relation [26]

$$\langle \mathcal{O} \rangle_{\text{real}} = \frac{\langle \psi_0 | \mathcal{O} | \psi_0 \rangle}{\langle \psi_0 | \psi_0 \rangle} = \frac{\left( \frac{\langle \psi_T | \mathcal{O} | \psi_0 \rangle}{\langle \psi_T | \psi_0 \rangle} \right)^2}{\frac{\langle \psi_T | \mathcal{O} | \psi_T \rangle}{\langle \psi_T | \psi_T \rangle}} = \frac{\langle \mathcal{O} \rangle_{\text{DMC}}^2}{\langle \mathcal{O} \rangle_{\text{VMC}}}, \quad (41)$$

where  $\psi_T$  is the trial wave function and  $\psi_0$  the projected ground state wave function. Although easy to implement, the calculation of single-particle densities in the present version of the AFDMC algorithm suffers of two main issues. On one hand, the employed trial wave function is too poor for variational calculations. The estimate of  $\langle \mathcal{O} \rangle_{\text{VMC}}$  could be not accurate enough, introducing severe biases in the calculation of  $\langle \mathcal{O} \rangle_{\text{real}}$ . On the other hand, the employed  $NN$  potential is too simplified to correctly describe the physics of nucleons in nuclei and hypernuclei, particularly for heavy systems. This lack of accuracy does not affect the calculation of the hyperon separation energy but could be important in the estimate of single particle densities. For these reasons we do not report here the results for nucleon and hyperon single-particle densities which will be presented in a future work in connection with a better trial wave function and a more realistic nucleon-nucleon interaction.

## B. Double $\Lambda$ hypernuclei

In the case of double  $\Lambda$  hypernuclei, the interesting observables we can access with the AFDMC are the double  $\Lambda$  separation energy,

$$B_{\Lambda\Lambda}({}^A_{\Lambda\Lambda}\text{Z}) = E({}^{A-2}\text{Z}) - E({}^A_{\Lambda\Lambda}\text{Z}), \quad (42)$$

and the incremental  $\Lambda\Lambda$  energy,

$$\Delta B_{\Lambda\Lambda}({}^A_{\Lambda\Lambda}\text{Z}) = B_{\Lambda\Lambda}({}^A_{\Lambda\Lambda}\text{Z}) - 2B_{\Lambda}({}^{A-1}_{\Lambda}\text{Z}). \quad (43)$$

The calculation of these quantities proceeds in the same way of those for single  $\Lambda$  hypernuclei, starting from the energy

TABLE VI. Comparison between  ${}^4\text{He}$  and the corresponding single and double  $\Lambda$  hypernuclei. In the second column the total energies are reported. The third column shows the single or double  $\Lambda$  separation energies. In the last column the incremental  $\Lambda\Lambda$  energy  $\Delta B_{\Lambda\Lambda}$  is reported. All the results are obtained using the complete two- plus three-body [set (II)] hyperon-nucleon interaction with the addition of the  $\Lambda\Lambda$  force of Eq. (17). The results are expressed in MeV.

System	$E$	$B_{\Lambda(\Lambda)}$	$\Delta B_{\Lambda\Lambda}$
${}^4\text{He}$	-32.67(8)		
${}^5_{\Lambda}\text{He}$	-35.89(12)	3.22(14)	
${}^6_{\Lambda\Lambda}\text{He}$	-40.6(3)	7.9(3)	1.5(4)
${}^6_{\Lambda\Lambda}\text{He}$	Expt. [16]	$7.25 \pm 0.19^{+0.18}_{-0.11}$	$1.01 \pm 0.20^{+0.18}_{-0.11}$

of the nucleus, the corresponding  $\Lambda$  hypernucleus and now the double  $\Lambda$  hypernucleus. In Table VI, we report the total energies for  ${}^4\text{He}$ ,  ${}^5_{\Lambda}\text{He}$ , and  ${}^6_{\Lambda\Lambda}\text{He}$  in the second column, the single or double hyperon separation energies in the third and the incremental  $\Lambda\Lambda$  energy in the last column. The value of  $B_{\Lambda\Lambda}$  confirms the weak attractive nature of the  $\Lambda\Lambda$  interaction [48,52–54]. Starting from  ${}^4\text{He}$  and adding two hyperons with  $B_{\Lambda} = 3.22(14)$  MeV, the energy of  ${}^6_{\Lambda\Lambda}\text{He}$  would be 1.0 to 1.5 MeV less than the actual AFDMC result. Therefore the  $\Lambda\Lambda$  potential of Eq. (17) induces a net attraction between hyperons, at least at this density.

Our results for  $B_{\Lambda\Lambda}$  and  $\Delta B_{\Lambda\Lambda}$  are very close to the expected results for which the potential has originally been fitted within the cluster model. The latest results  $B_{\Lambda\Lambda} = 6.91(0.16)$  MeV and  $\Delta B_{\Lambda\Lambda} = 0.67(0.17)$  MeV of Ref. [23] suggest a weaker attractive force between the two hyperons. A refit of the interaction of the form proposed in Eq. (17) would be required. It would be interesting to study other double  $\Lambda$  hypernuclei within the AFDMC framework with the  $\Lambda N$ ,  $\Lambda NN$ , and  $\Lambda\Lambda$  interaction proposed. Some experimental data are available in the range  $A = 7$ –13, but there are uncertainties in the identification of the produced double  $\Lambda$  hypernuclei, reflecting in inconsistencies about the sign of the  $\Lambda\Lambda$  interaction [67,68]. An *ab initio* analysis of these systems might put some constraints on the hyperon-hyperon force, which at present is still poorly known, and give information on its density dependence. Also the inclusion of the  $\Lambda\Lambda N$  force would be important.

## V. CONCLUSIONS

We presented a detailed study of single  $\Lambda$  hypernuclei in the framework of the quantum Monte Carlo method. By accurately refitting the three-body hyperon-nucleon interaction we obtain substantial agreement with available experimental data. The present results confirm that the repulsion induced by the  $\Lambda NN$  force properly corrects the saturation property of the hyperon separation energy that is strongly overestimated by the use of a bare  $\Lambda N$  interaction.

A  $\Lambda\Lambda$  effective interaction has also been applied to the study of  ${}^6_{\Lambda\Lambda}\text{He}$ . Results are in good agreement with the available experimental data. This is a first step in the study of  $S = -2$   $\Lambda$  hypernuclei with QMC calculations, for which there are controversial results both from theoretical and experimental studies.

The three-body  $\Lambda NN$  interaction used in this work provides a stronger repulsion than in our previous more qualitative results. On the grounds of this observation, we feel confident that the application of the  $\Lambda N + \Lambda NN$  (and possibly  $\Lambda\Lambda$ ) interaction to the study of the homogeneous medium will lead to a stiff equation of state for the  $\Lambda$  neutron matter. This fact helps to understand how the necessary appearance of hyperons at some value of the nucleon density in the inner core of a neutron star might eventually be compatible with the observed neutron star masses of order  $2M_{\odot}$  [69,70]. A study along this direction is in progress and encouraging results are indeed already available.

## ACKNOWLEDGMENTS

This work has been partially performed at LISC, Interdisciplinary Laboratory for Computational Science, a joint venture of the University of Trento and Bruno Kessler Foundation. Support and computer time were partly made available by the AuroraScience project (funded by the Autonomous Province of Trento and INFN), and by Los Alamos Open Supercomputing. This research used also resources of the National Energy Research Scientific Computing Center, which is supported by the Office of Science of the US Department of Energy under Contract No. DE-AC02-05CH11231. The work of S.G. was supported by the Department of Energy Nuclear Physics Office, by the NUCLEI SciDAC program, and by a Los Alamos LDRD early career grant.

- 
- [1] V. G. J. Stoks, R. A. M. Klomp, M. C. M. Rentmeester, and J. J. de Swart, *Phys. Rev. C* **48**, 792 (1993).
- [2] V. G. J. Stoks, R. A. M. Klomp, C. P. F. Terheggen, and J. J. de Swart, *Phys. Rev. C* **49**, 2950 (1994).
- [3] R. B. Wiringa, V. G. J. Stoks, and R. Schiavilla, *Phys. Rev. C* **51**, 38 (1995).
- [4] R. Machleidt, F. Sammarruca, and Y. Song, *Phys. Rev. C* **53**, R1483 (1996).
- [5] R. B. Wiringa and S. C. Pieper, *Phys. Rev. Lett.* **89**, 182501 (2002).
- [6] E. Epelbaum, W. Glöckle, and U.-G. Meißner, *Nucl. Phys. A* **747**, 362 (2005).
- [7] A. Ekström, G. Baardsen, C. Forssén, G. Hagen, M. Hjorth-Jensen, G. R. Jansen, R. Machleidt, W. Nazarewicz, T. Papenbrock, J. Sarich, and S. M. Wild, *Phys. Rev. Lett.* **110**, 192502 (2013).
- [8] A. Gezerlis, I. Tews, E. Epelbaum, S. Gandolfi, K. Hebeler, A. Nogga, and A. Schwenk, *Phys. Rev. Lett.* **111**, 032501 (2013).
- [9] J. J. de Swart, M. M. Nagels, T. A. Rijken, and P. A. Verhoeven, in *Springer Tracts in Modern Physics*, Vol. 60 (Springer, Berlin, 1971), p. 138.
- [10] J. Kadyk, G. Alexander, J. Chan, P. Gaposchkin, and G. Trilling, *Nucl. Phys. B* **27**, 13 (1971).

- [11] J. Ahn, H. Akikawa, J. Arvieux, B. Bassalleck, M. Chung, H. En'yo, T. Fukuda, H. Funahashi, S. Golovkin, A. Gorin, Y. Goto, M. Hanabata, T. Hayakawa, A. Ichikawa, M. Ieiri, K. Imai, M. Ishino, H. Kanda, Y. Kim, Y. Kondo, E. Kozarenko, I. Kreslo, J. Lee, A. Masaike, S. Mihara, K. Nakai, K. Nakazawa, K. Ozawa, A. Sato, H. Sato, K. Sim, T. Tabaru, F. Takeuchi, P. Tlustý, H. Torii, K. Yamamoto, S. Yokkaichi, and M. Yoshida, *Nucl. Phys. A* **761**, 41 (2005).
- [12] M. Jurič, G. Bohm, J. Klubuhn, U. Krecker, F. Wysotzki, G. Coremans-Bertrand, J. Sacton, G. Wilquet, T. Cantwell, F. Esmael, A. Montwill, D. H. Davis, D. Kielczewska, T. Pniewski, T. Tymieniecka, and J. Zakrzewski, *Nucl. Phys. B* **52**, 1 (1973).
- [13] T. Cantwell, D. Davis, D. Kielczewska, J. Zakrzewski, M. Jurič, U. Krecker, G. Coremans-bertrand, J. Sacton, T. Tymieniecka, A. Montwill, and P. Moriarty, *Nucl. Phys. A* **236**, 445 (1974).
- [14] P. H. Pile, S. Bart, R. E. Chrien, D. J. Millener, R. J. Sutter, N. Tsoupas, J.-C. Peng, C. S. Mishra, E. V. Hungerford, T. Kishimoto, L.-G. Tang, W. von Witsch, Z. Xu, K. Maeda, D. Gill, R. McCrady, B. Quinn, J. Seydoux, J. W. Sleight, R. L. Stearns, H. Plendl, A. Rafatian, and J. Reidy, *Phys. Rev. Lett.* **66**, 2585 (1991).
- [15] T. Hasegawa, O. Hashimoto, S. Homma, T. Miyachi, T. Nagae, M. Sekimoto, T. Shibata, H. Sakaguchi, T. Takahashi, K. Aoki, H. Noumi, H. Bhang, M. Youn, Y. Gavrilov, S. Ajimura, T. Kishimoto, A. Ohkusu, K. Maeda, R. Sawafta, and R. P. Redwine, *Phys. Rev. C* **53**, 1210 (1996).
- [16] H. Takahashi, J. Ahn, H. Akikawa, S. Aoki, K. Arai, S. Bahk, K. Baik, B. Bassalleck, J. Chung, M. Chung, D. Davis, T. Fukuda, K. Hoshino, A. Ichikawa, M. Ieiri, K. Imai, Y. Iwata, H. Kanda, M. Kaneko, T. Kawai, M. Kawasaki, C. Kim, J. Kim, S. Kim, Y. Kondo, T. Kouketsu, Y. Lee, J. McNabb, M. Mitsuhashi, Y. Nagase, C. Nagoshi, K. Nakazawa, H. Noumi, S. Ogawa, H. Okabe, K. Oyama, H. Park, I. Park, J. Parker, Y. Ra, J. Rhee, A. Rusek, H. Shibuya, K. Sim, P. Saha, D. Seki, M. Sekimoto, J. Song, T. Takahashi, F. Takeuchi, H. Tanaka, K. Tanida, J. Tojo, H. Torii, S. Torikai, D. Tovee, N. Ushida, K. Yamamoto, N. Yasuda, J. Yang, C. Yoon, M. Yosoi, T. Yoshida, and L. Zhu, *Phys. Rev. Lett.* **87**, 212502 (2001).
- [17] L. Yuan, M. Sarsour, T. Miyoshi, X. Zhu, A. Ahmidouch, D. Androic, T. Angelescu, R. Asaturyan, S. Avery, O. Baker, I. Bertovic, H. Breuer, R. Carlini, J. Cha, R. Chrien, M. Christy, L. Cole, S. Danagoulian, D. Dehnhard, M. Elaasar, A. Empl, R. Ent, H. Fenker, Y. Fujii, M. Furic, L. Gan, K. Garrow, A. Gasparian, P. Gueye, M. Harvey, O. Hashimoto, W. Hinton, B. Hu, E. Hungerford, C. Jackson, K. Johnston, H. Juengst, C. Keppel, K. Lan, Y. Liang, V. Likhachev, J. Liu, D. Mack, A. Margaryan, P. Markowitz, H. Mkrtchyan, S. Nakamura, T. Petkovic, J. Reinhold, J. Roche, Y. Sato, R. Sawafta, N. Simicevic, G. Smith, S. Stepanyan, R. Sutter, V. Tadevosyan, T. Takahashi, K. Tanida, L. Tang, M. Ukai, A. Uzzle, W. Vulcan, S. Wells, S. Wood, G. Xu, H. Yamaguchi, and C. Yan, *Phys. Rev. C* **73**, 044607 (2006).
- [18] F. Cusanno, G. Urciuoli, A. Acha, P. Ambrozewicz, K. Aniol, P. Baturin, P. Bertin, H. Benaoum, K. Blomqvist, W. Boeglin, H. Breuer, P. Brindza, P. Bydžovský, A. Camsonne, C. Chang, J.-P. Chen, S. Choi, E. Chudakov, E. Cisbani, S. Colilli, L. Coman, B. Craver, G. De Cataldo, C. de Jager, R. De Leo, A. Deur, C. Ferdi, R. Feuerbach, E. Folts, R. Fratoni, S. Frullani, F. Garibaldi, O. Gayou, F. Giuliani, G. Gomez, M. Gricia, J. Hansen, D. Hayes, D. Higinbotham, T. Holmstrom, C. Hyde, H. Ibrahim, M. Iodice, X. Jiang, L. Kaufman, K. Kino, B. Kross, L. Lagamba, J. LeRose, R. Lindgren, M. Lucentini, D. Margaziotis, P. Markowitz, S. Marrone, Z. Mezziani, K. McCormick, R. Michaels, D. Millener, T. Miyoshi, B. Moffit, P. Monaghan, M. Moteabbed, C. Muñoz Camacho, S. Nanda, E. Nappi, V. Nelyubin, B. Norum, Y. Okasyasu, K. Paschke, C. Perdrisat, E. Piassetzky, V. Punjabi, Y. Qiang, B. Raue, P. Reimer, J. Reinhold, B. Reitz, R. Roche, V. Rodriguez, A. Saha, F. Santavenere, A. Sarty, J. Segal, A. Shahinyan, J. Singh, S. Širca, R. Snyder, P. Solvignon, M. Sotona, R. Subedi, V. Sulkosky, T. Suzuki, H. Ueno, P. Ulmer, P. Veneroni, E. Voutier, B. Wojtsekhowski, X. Zheng, and C. Zorn, *Phys. Rev. Lett.* **103**, 202501 (2009).
- [19] M. Agnello, L. Benussi, M. Bertani, H. C. Bhang, G. Bonomi, E. Botta, M. Bregant, T. Bressani, S. Bufalino, L. Busso, D. Calvo, P. Camerini, B. Dalena, F. De Mori, G. D'Erasmus, F. L. Fabbri, A. Feliciello, A. Filippi, E. M. Fiore, A. Fontana, H. Fujioka, P. Genova, P. Gianotti, N. Grion, B. Kang, V. Lucherini, S. Marcello, F. Moia, T. Maruta, N. Mirfakhrai, P. Montagna, O. Morra, T. Nagae, D. Nakajima, H. Outa, A. Pantaleo, V. Paticchio, S. Piano, R. Rui, G. Simonetti, A. Toyoda, R. Wheadon, and A. Zenoni, *Nucl. Phys. A* **835**, 414 (2010).
- [20] K. Nakazawa, *Nucl. Phys. A* **835**, 207 (2010).
- [21] M. Agnello, L. Benussi, M. Bertani, H. Bhang, G. Bonomi, E. Botta, M. Bregant, T. Bressani, S. Bufalino, L. Busso, D. Calvo, P. Camerini, B. Dalena, F. De Mori, G. D'Erasmus, F. L. Fabbri, A. Feliciello, A. Filippi, E. M. Fiore, A. Fontana, H. Fujioka, P. Genova, P. Gianotti, N. Grion, V. Lucherini, S. Marcello, N. Mirfakhrai, F. Moia, O. Morra, T. Nagae, H. Outa, A. Pantaleo, V. Paticchio, S. Piano, R. Rui, G. Simonetti, R. Wheadon, A. Zenoni, and A. Gal (FINUDA Collaboration), *Phys. Rev. Lett.* **108**, 042501 (2012).
- [22] S. Nakamura, A. Matsumura, Y. Okayasu, T. Seva, V. Rodriguez, P. Baturin, L. Yuan, A. Acha, A. Ahmidouch, D. Androic, A. Asaturyan, R. Asaturyan, O. Baker, F. Benmokhtar, P. Bosted, R. Carlini, C. Chen, M. Christy, L. Cole, S. Danagoulian, A. Daniel, V. Dharmawardane, K. Egiyan, M. Elaasar, R. Ent, H. Fenker, Y. Fujii, M. Furic, L. Gan, D. Gaskell, A. Gasparian, E. Gibson, T. Gogami, P. Gueye, Y. Han, O. Hashimoto, E. Hiyama, D. Honda, T. Horn, B. Hu, E. Hungerford, C. Jayalath, M. Jones, K. Johnston, N. Kalantarians, H. Kanda, M. Kaneta, F. Kato, S. Kato, D. Kawama, C. Keppel, K. Lan, W. Luo, D. Mack, K. Maeda, S. Malace, A. Margaryan, G. Marikyan, P. Markowitz, T. Maruta, N. Maruyama, T. Miyoshi, A. Mkrtchyan, H. Mkrtchyan, S. Nagao, T. Navasardyan, G. Niculescu, M.-I. Niculescu, H. Nomura, K. Nonaka, A. Ohtani, M. Oyamada, N. Perez, T. Petkovic, S. Randeniya, J. Reinhold, J. Roche, Y. Sato, E. Segbefia, N. Simicevic, G. Smith, Y. Song, M. Sumihama, V. Tadevosyan, T. Takahashi, L. Tang, K. Tsukada, V. Tvaskis, W. Vulcan, S. Wells, S. Wood, C. Yan, and S. Zhamkochyan (HKS (JLab E01-011) Collaboration), *Phys. Rev. Lett.* **110**, 012502 (2013).
- [23] J. K. Ahn, H. Akikawa, S. Aoki, K. Arai, S. Y. Bahk, K. M. Baik, B. Bassalleck, J. H. Chung, M. S. Chung, D. H. Davis, T. Fukuda, K. Hoshino, A. Ichikawa, M. Ieiri, K. Imai, K. Itonaga, Y. H. Iwata, Y. S. Iwata, H. Kanda, M. Kaneko, T. Kawai, M. Kawasaki, C. O. Kim, J. Y. Kim, S. H. Kim, S. J. Kim, Y. Kondo, T. Kouketsu, H. N. Kyaw, Y. L. Lee, J. W. C. McNabb, A. A. Min, M. Mitsuhashi, K. Miwa, K. Nakazawa, Y. Nagase, C. Nagoshi, Y. Nakanishi, H. Noumi, S. Ogawa, H. Okabe, K. Oyama, B. D. Park, H. M. Park, I. G. Park, J. Parker, Y. S. Ra, J. T. Rhee, A. Rusek, A. Sawa, H. Shibuya, K. S. Sim, P. K. Saha,

- D. Seki, M. Sekimoto, J. S. Song, H. Takahashi, T. Takahashi, F. Takeuchi, H. Tanaka, K. Tanida, K. T. Tint, J. Tojo, H. Torii, S. Torikai, D. N. Tovee, T. Tsunemi, M. Ukai, N. Ushida, T. Wint, K. Yamamoto, N. Yasuda, J. T. Yang, C. J. Yoon, C. S. Yoon, M. Yosoi, T. Yoshida, and L. Zhu (E373 (KEK-PS) Collaboration), *Phys. Rev. C* **88**, 014003 (2013).
- [24] A. Feliciello, *Mod. Phys. Lett. A* **28**, 1330029 (2013).
- [25] D. Lonardoni, S. Gandolfi, and F. Pederiva, *Phys. Rev. C* **87**, 041303 (2013).
- [26] S. C. Pieper, *Nuovo Cimento Riv. Se.* **31**, 709 (2008).
- [27] D. Lonardoni, F. Pederiva, and S. Gandolfi, in XI International Conference on Hypernuclear and Strange Particle Physics (HYP2012) [*Nucl. Phys. A* **914**, 243 (2013)].
- [28] A. R. Bodmer, Q. N. Usmani, and J. Carlson, *Phys. Rev. C* **29**, 684 (1984).
- [29] A. R. Bodmer and Q. N. Usmani, *Phys. Rev. C* **31**, 1400 (1985).
- [30] A. Bodmer and Q. Usmani, *Nucl. Phys. A* **477**, 621 (1988).
- [31] A. A. Usmani, S. C. Pieper, and Q. N. Usmani, *Phys. Rev. C* **51**, 2347 (1995).
- [32] M. Shoeb, Q. Usmani, and A. Bodmer, *Pramana* **51**, 421 (1998).
- [33] M. Shoeb, N. Neelofer, Q. N. Usmani, and M. Z. Rahman Khan, *Phys. Rev. C* **59**, 2807 (1999).
- [34] Q. N. Usmani and A. R. Bodmer, *Phys. Rev. C* **60**, 055215 (1999).
- [35] R. Sinha, Q. N. Usmani, and B. M. Taib, *Phys. Rev. C* **66**, 024006 (2002).
- [36] A. A. Usmani and S. Murtaza, *Phys. Rev. C* **68**, 024001 (2003).
- [37] Q. N. Usmani, A. R. Bodmer, and B. Sharma, *Phys. Rev. C* **70**, 061001(R) (2004).
- [38] M. Shoeb, *Phys. Rev. C* **69**, 054003(R) (2004).
- [39] A. A. Usmani, *Phys. Rev. C* **73**, 011302(R) (2006).
- [40] A. A. Usmani and Z. Hasan, *Phys. Rev. C* **74**, 034320 (2006).
- [41] A. A. Usmani and F. C. Khanna, *J. Phys. G: Nucl. Part. Phys.* **35**, 025105 (2008).
- [42] S. Shinmura, Y. Akaishi, and H. Tanaka, *Prog. Theor. Phys.* **71**, 546 (1984).
- [43] I. Lagaris and V. Pandharipande, *Nucl. Phys. A* **359**, 331 (1981).
- [44] A. R. Bodmer and D. Rote, *Nucl. Phys. A* **169**, 1 (1971).
- [45] J. Rozynek and J. Dabrowski, *Phys. Rev. C* **20**, 1612 (1979).
- [46] A. A. Usmani, *Phys. Rev. C* **52**, 1773 (1995).
- [47] E. Hiyama, M. Kamimura, T. Motoba, T. Yamada, and Y. Yamamoto, *Prog. Theor. Phys.* **97**, 881 (1997).
- [48] E. Hiyama, M. Kamimura, T. Motoba, T. Yamada, and Y. Yamamoto, *Phys. Rev. C* **66**, 024007 (2002).
- [49] I. N. Filikhin and A. Gal, *Phys. Rev. C* **65**, 041001 (2002).
- [50] M. Shoeb, *Phys. Rev. C* **71**, 024004 (2005).
- [51] M. Shoeb, A. Mamo, and A. Fessahatsion, *Pramana* **68**, 943 (2007).
- [52] M. M. Nagels, T. A. Rijken, and J. J. de Swart, *Phys. Rev. D* **20**, 1633 (1979).
- [53] P. M. M. Maessen, T. A. Rijken, and J. J. de Swart, *Phys. Rev. C* **40**, 2226 (1989).
- [54] T. A. Rijken, V. G. J. Stoks, and Y. Yamamoto, *Phys. Rev. C* **59**, 21 (1999).
- [55] K. E. Schmidt and S. Fantoni, *Phys. Lett. B* **446**, 99 (1999).
- [56] S. C. Pieper, *Nucl. Phys. A* **751**, 516 (2005).
- [57] E. Lusk, S. C. Pieper, and R. Butler, *SciDAC Rev.* **17**, 30 (2010).
- [58] A. Lovato, S. Gandolfi, R. Butler, J. Carlson, E. Lusk, S. C. Pieper, and R. Schiavilla, *Phys. Rev. Lett.* **111**, 092501 (2013).
- [59] S. Gandolfi, J. Carlson, and S. C. Pieper, *Phys. Rev. Lett.* **106**, 012501 (2011).
- [60] S. Gandolfi, F. Pederiva, S. Fantoni, and K. E. Schmidt, *Phys. Rev. C* **73**, 044304 (2006).
- [61] S. Gandolfi, F. Pederiva, S. Fantoni, and K. E. Schmidt, *Phys. Rev. Lett.* **99**, 022507 (2007).
- [62] S. Gandolfi, A. Y. Illarionov, K. E. Schmidt, F. Pederiva, and S. Fantoni, *Phys. Rev. C* **79**, 054005 (2009).
- [63] X. Bai and J. Hu, *Phys. Rev. C* **56**, 1410 (1997).
- [64] S. C. Pieper, V. R. Pandharipande, R. B. Wiringa, and J. Carlson, *Phys. Rev. C* **64**, 014001 (2001).
- [65] O. Hashimoto and H. Tamura, *Progr. Part. Nucl. Phys.* **57**, 564 (2006).
- [66] H. Hotchi, T. Nagaie, H. Oota, H. Noumi, M. Sekimoto, T. Fukuda, H. Bhang, Y. D. Kim, J. H. Kim, H. Park, K. Tanida, O. Hashimoto, H. Tamura, T. Takahashi, Y. Sato, T. Endo, S. Satoh, J. Nishida, T. Miyoshi, T. Saitoh, T. Kishimoto, A. Sakaguchi, S. Ajimura, Y. Shimizu, T. Mori, S. Minami, M. Sumihama, R. Sawafta, and L. Tang, *Phys. Rev. C* **64**, 044302 (2001).
- [67] C. Dover, D. Millener, A. Gal, and D. Davis, *Phys. Rev. C* **44**, 1905 (1991).
- [68] Y. Yamamoto, H. Takaki, and K. Ikeda, *Prog. Theor. Phys.* **86**, 867 (1991).
- [69] P. B. Demorest, T. Pennucci, S. M. Ransom, M. S. E. Roberts, and J. W. T. Hessels, *Nature (London)* **467**, 1081 (2010).
- [70] J. Antoniadis, P. C. C. Freire, N. Wex, T. M. Tauris, R. S. Lynch, M. H. van Kerkwijk, M. Kramer, C. Bassa, V. S. Dhillon, T. Driebe, J. W. T. Hessels, V. M. Kaspi, V. I. Kondratiev, N. Langer, T. R. Marsh, M. A. McLaughlin, T. T. Pennucci, S. M. Ransom, I. H. Stairs, J. van Leeuwen, J. P. W. Verbiest, and D. G. Whelan, *Science* **340**, 1233232 (2013).